BRIEF REPORTS

Brief Reports are accounts of completed research which do not warrant regular articles or the priority handling given to Rapid Communications; however, the same standards of scientific quality apply. (Addenda are included in Brief Reports.) A Brief Report may be no longer than 4 printed pages and must be accompanied by an abstract. The same publication schedule as for regular articles is followed, and page proofs are sent to authors.

Correlated photon asymmetry in local realism

Stuart Mirell
Nuclear Medicine Service W115, Veterans Affairs Medical Center West Los Angeles, Los Angeles, California 90073 and Department of Radiological Sciences, School of Medicine, University of California, Los Angeles, California 90024*
(Received 7 January 1994)

Agreement with quantum theory and experiment exists for locally real models violating the apparently plausible additional assumptions of Bell inequalities subject to the use of low-efficiency detectors. A locally real optical hidden-variable model of this class is constructed here with asymmetric correlated photon pairs from the physical basis of Malus's law. The model introduces no arbitrary constants, naturally violates factorization and no enhancement, predicts a $\frac{1}{3}\cos^2\theta$ joint probability for high-efficiency detectors, and is testable with currently available low-efficiency detectors.

PACS number(s): 03.65.Bz

A diversity of local realities has been represented by hidden-variable theories [1] that violate the additional assumptions associated with Bell's inequalities [2–4]. These theories agree with performed experiments using low-efficiency detectors [5]. This diversity and the apparent plausibility of the additional assumptions motivate the present work.

A model of local reality is developed here with the vacuum field treated as a collection of harmonic oscillators in random ground-state motion. Photons comprise a set of propagating planar Fourier ground-state wave packets on which the oscillators are in coherent ground-state motion. These planar packets are contiguously arrayed about the propagation axis, each occupying a discrete infinitesimal angular arc $\delta \ll \pi$ (Fig. 1). A large δ is depicted in the figures for clarity; however, the functional quantities developed in the model remain valid as $\delta \to 0$.

Collectively, a photon's packets subtend an arc of specific angular magnitude about its propagation axis. The arc bisector defines the orientation angle λ of a photon in the laboratory reference frame K. (Planar packet bidirectionality gives orientation a bivalue of λ and $\lambda+\pi$.) The maximum permissible arc magnitude is $\pi/2$ and this particular case is defined as a "full-complement" photon.

In the interests of conciseness, the underlying field structure of the model, which is compatible with the formalism of quantum theory, is deferred here, and the essentials of the model are presented in their most compact form as a hidden-variable theory. In this context, the arc magnitude and orientation of a photon constitute the requisite hidden variables.

In the model, an analyzer with its polarization axis oriented at θ_0 in K transmits a photon only when any region of its arc is aligned with that θ_0. Then the transmission probability is $\frac{1}{2}$ for a randomly oriented full-complement photon γ (and, e.g., $\frac{1}{3}$ for a randomly oriented γ with a $\pi/3$ arc). If no portion of the arc is aligned with the polarization axis, all packets collapse and the photon is absorbed. Conversely, a transmitted photon collapses down to the single packet aligned with the polarization axis as it enters the analyzer. This single-packet "generator" photon γ_g, aligned with the polarization axis, propagates in the analyzer and emerges at the analyzer exit face as a full-complement "emission" photon γ_e.

The energy associated with a photon resides as an exci-

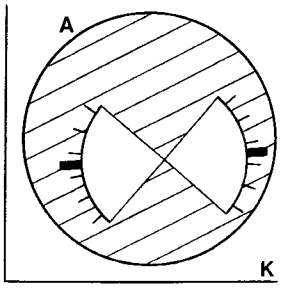

FIG. 1. Schematic view of a full-complement photon γ incident on an analyzer A. The depicted γ is transmitted since a constituent packet is aligned with the analyzer's polarization axis.

*Address for correspondence.

 ©1994 The American Physical Society

tation state on one of the oscillators of one of the constituent packets. When a photon incident on an analyzer is transmitted, the excitation transfers to the internally transmitted single packet of γ_g during the collapse of the other packets. The excitation subsequently transfers to one of the packets of the full-complement γ_e photon emitted at the analyzer exit face.

The distribution of the possible orientations of that emission photon γ_e is stochastically related to the (analyzer-dependent) orientation of the generator photon γ_g. An emitted γ_e is a random member of an ensemble $\{\gamma_e\}$. The ensemble is given by the curvilinear envelope $\cos^2\lambda'$ for $0<\lambda'<\pi/2$, $1-\cos^2\lambda'$ for $-\pi/2<\lambda'<0$, and connecting horizontal segments (Fig. 2) where the analyzer axis and its internally propagating single-packet photon γ_g have an orientation defined to be $\lambda'=0$ in the photon reference frame K' of γ_g. The ensemble distribution in Fig. 2 is chosen in the model because it uniquely weights the ensemble member orientations by $\cos^2\lambda'$ about the orientation of γ_g and suffices to provide a local basis for Malus's law. (A subsequent analyzer at $\lambda'=\theta$ transmits $\cos^2\theta$ of the ensemble members.)

Correlated photons are treated analogously as pairs consisting of a "generator" photon γ_G and its stochastically dependent "emission" photon γ_E. The γ_G and the γ_E are asymmetric with respect to structural proportion. The γ_G is distinctive in having a $\pi/3$ arc of packets, whereas the γ_E (and in general other γ's such as uncorrelated photons as well as the γ_e) have a full complement $\pi/2$ arc. The γ_G photons then comprise a packet set $\frac{2}{3}$ as numerous as that of a full-complement set. The γ_g is physically confined to a single-packet structure by the analyzer, whereas this constraint is absent for the analogous γ_G. (The particular choice of a $\pi/3$ arc for γ_G is examined below.)

A $\gamma_G(\lambda)$, upon leaving a correlated photon source S, may assume any orientation λ in K with equal probability. However, it is more convenient to transform to the generator photon reference frame K' where the γ_G orientation is fixed at $\lambda'=0$. Associated with γ_G is an ensemble $\{\gamma_E\}$ comprising members $\gamma_E(\lambda')$, where λ' identifies the orientation in K' of each member (Fig. 3). The particular $\gamma_E(\lambda')$ emitted with a γ_G is a random member of that $\{\gamma_E\}$. In K', an analyzer orientation θ_0 may assume any value of λ' with equal probability since γ_G is fixed at $\lambda'=0$. The probability of transmitting a random $\{\gamma_E\}$ member through an analyzer set at some λ' (e.g., $=\theta_R$) is given by

$$P_E(\lambda')=\begin{cases}(3/\pi)(\pi/3-\lambda')6/\pi, & \pi/6\le\lambda',\le\pi/3\\ 3/\pi, & |\lambda'|\le\pi/6\\ (3/\pi)(\pi/3+\lambda')6/\pi, & -\pi/3\le\lambda'\le-\pi/6\\ 0, & \pi/3\le|\lambda'|\le2\pi/3\ .\end{cases} \tag{1}$$

The $3/\pi$ factor provides for necessary normalization.

The corresponding probability of γ_G being transmitted by a different analyzer at some λ' (e.g., $=\theta_L$) is

$$P_G(\lambda')=\begin{cases}1, & |\lambda'|\le\pi/6\\ 0, & \pi/6<|\lambda'|<5\pi/6\ .\end{cases} \tag{2}$$

A gedanken EPR (Einstein-Podolsky-Rosen) [6] correlated photon experiment may now be performed. The requisite apparatus comprises a correlated photon source S situated between a polarization analyzer A_L on the left and a polarization analyzer A_R on the right. Each analyzer is followed by an associated detector. The coincidence rate for the experiment is then

$$R(\theta)=\tfrac{1}{2}R_T f(\tfrac{1}{3})\left[\int_\Lambda P_G(\theta_L)P_E(\theta_R)d\lambda'\right]\eta^2 + \tfrac{1}{2}R_T f(\tfrac{1}{3})[\int_\Lambda P_G(\theta_R)P_E(\theta_L)d\lambda']\eta^2\ , \tag{3}$$

where $\theta=\theta_R-\theta_L$ is the relative angular displacement of A_R and A_L. The analysis is performed in K'. Idealizations are made with respect to correlated photon production (e.g., energy equivalence), trajectory correlation, and analyzer performance.

The factors in the first term on the right are examined. The $\frac{1}{2}$ factor expresses the probability that γ_G travels to

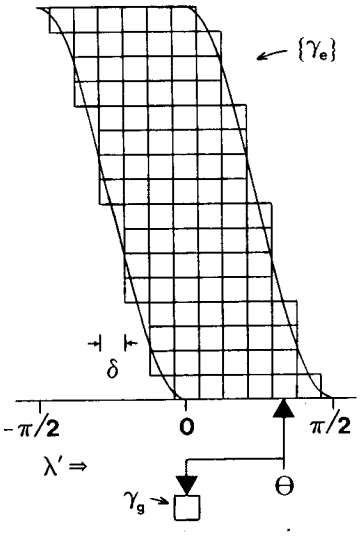

FIG. 2. Angular relationship of a single packet γ_g, propagating in an analyzer, and its associated ensemble $\{\gamma_e\}$, shown in the reference frame K' of γ_g. The particular γ_e emitted at the analyzer exit face in a random member (row) of $\{\gamma_e\}$.

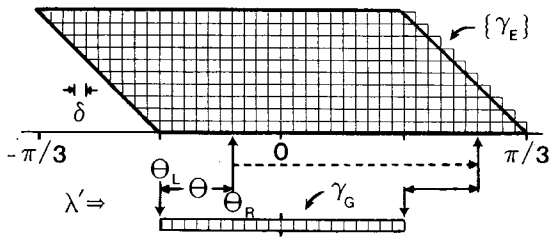

FIG. 3. Packet distributions of the γ_G correlated photon and its associated ensemble $\{\gamma_E\}$ in the angular reference frame K' of γ_G. A γ_E mate to a γ_G is a random row in $\{\gamma_E\}$. Left and right analyzers at θ_L and θ_R for all λ' in K' give transmission probabilities (shown here, γ_G moving left and γ_E moving right).

the left and γ_E to the right for this term. R_T is the true production rate of correlated photons from S. The factor f is the fractional angular acceptance cone of the analyzer-detector sets. The $\frac{1}{3}$ factor is the probability of γ_G being transmitted by analyzer A_L. The corresponding probability of an associated γ_E being transmitted by A_R set at $\theta_R=\lambda'$, subject to the constraint of γ_G being transmitted by A_L set at θ_L, is given by the integral of P_G and P_E. However, this constraint demands that the integration variable of P_G be displaced by θ since $\theta=\theta_R-\theta_L$. Then for the integral under consideration, $\theta_L=\lambda'-\theta$ and (2) becomes

$$P_G(\lambda'-\theta)=\begin{cases}1, & |\lambda'-\theta|\le\pi/6\\ 0, & \pi/6<|\lambda'-\theta|<5\pi/6\end{cases}. \tag{4}$$

Integration of (1) and (4) over $[-\pi/2,\pi/2]$ may now be performed (Fig. 3). The nonzero contributions to the integral resolve to that range Λ (dashed line) for which θ_L intercepts the arc of γ_G, and θ_R simultaneously intercepts the nonzero portion of the distribution $P_E(\lambda')$ (1) of $\{\gamma_E\}$. Defining $C(\theta)$ as the integral in the first term of (3),

$$C(\theta)=\frac{3}{\pi}\int_{\theta-\pi/6}^{\pi/6}d\lambda'+\frac{3}{\pi}\int_{\pi/6}^{\theta+\pi/6}\left|\frac{\pi}{3}-\lambda'\right|\frac{6}{\pi}d\lambda'$$
$$=1-\left[\frac{3\theta}{\pi}\right]^2, \tag{5}$$

$$C(\theta)=\frac{3}{\pi}\int_{\theta-\pi/6}^{\pi/6}d\lambda'+\frac{3}{\pi}\int_{\pi/6}^{\pi/3}\left|\frac{\pi}{3}-\lambda'\right|\frac{6}{\pi}d\lambda'$$
$$=1.25-\frac{3\theta}{\pi}, \tag{6}$$

$$C(\theta)=\frac{3}{\pi}\int_{\theta-\pi/6}^{\pi/3}\left|\frac{\pi}{3}-\lambda'\right|\frac{6}{\pi}d\lambda'$$
$$=2.25-\frac{9\theta}{\pi}+\left[\frac{3\theta}{\pi}\right]^2, \tag{7}$$

respectively, for $0\le\theta\le\pi/6$, $\pi/6\le\theta\le\pi/3$, and $\pi/3\le\theta\le\pi/2$. Examination of $C(\theta)$ over $[0,\pi/2]$ shows excellent agreement with $\cos^2\theta$, i.e., $C(\theta)\approx\cos^2\theta$. The particular choice of a $\pi/3$ arc for γ_G maximizes this agreement. This maximized agreement is, in turn, required in the model that treats correlated photon ensembles $\{\gamma_E\}$ as physically analogous to the analyzer ensembles $\{\gamma_e\}$. In this analogy the $\cos^2\theta$ proportion of all $\{\gamma_e\}$ members having a packet at θ from the single packet γ_g, is equivalent to the $C(\theta)$ normalized proportion of all $\{\gamma_E\}$ members having a packet at θ from a particular packet in γ_G integrated over the multiple γ_G packets. As a result, the $\pi/3$ arc of γ_G is a derived constant.

With η as detector efficiency for full-complement photons and noting that γ_G and γ_E are both full complement after transmission through their respective analyzers, the final factor is η^2.

The second term on the right of Eq. (3), relating to γ_G propagating to the right and γ_E propagating to the left, is equivalent to the first term by symmetry. It follows that

$$R(\theta)=\tfrac{1}{3}R_T f\eta^2 C(\theta)\ . \tag{8}$$

Without the analyzers, the detection rate is

$$R_0=R_T f\eta_G\eta\ , \tag{9}$$

where η_G is the detection efficiency for the γ_G. The ratio of Eqs. (8) and (9) is

$$\frac{R(\theta)}{R_0}=\frac{\eta^2 C(\theta)}{3\eta_G\eta}\ . \tag{10}$$

The arc magnitude of a photon presents a proportionate cross section of interaction. Detection efficiency is linear to this magnitude and $\eta_G=\frac{2}{3}\eta$. Eq. (10) reduces to

$$\frac{R(\theta)}{R_0}=\tfrac{1}{2}C(\theta)\approx\tfrac{1}{2}\cos^2\theta\ , \tag{11}$$

which is the familiar form of the joint probability.

Arc-dependent detection efficiency is a significant outcome of the model. The γ_G and γ_E, equal in energy, nevertheless exhibit detection efficiencies linearly proportionate to their respective arc magnitudes ("linearity").

Equation (11) expresses the mutual agreement of quantum theory and performed experiments with the model. However, this agreement is comparable to that obtained with other locally real models using low-efficiency detectors [1]. The aspects that distinguish the present model from those models are examined below.

The computation of the joint probability Eq. (11) is critically dependent upon linearity, which is taken to be the defining characteristic of low-efficiency detectors. Upon considering progressively improved detectors, it is evident that as η_G for γ_G photons approaches unity, η must also converge to unity. The consequent departure from linearity (i.e., from low efficiency) results in $\eta_G>\frac{2}{3}\eta$ for which

$$\frac{R(\theta)}{R_0}<\tfrac{1}{2}C(\theta)\approx\tfrac{1}{2}\cos^2\theta\ , \tag{12}$$

and the model predicts that quantum theory will be at variance with experiment. This variance necessarily must exist at least for $\eta_G>\frac{2}{3}$ since linearity would require $\eta>1$. Then the maximum limit of low efficiency is $\eta_G=\frac{2}{3}$ and $\eta=1$. In this limit, a γ_G,γ_E flux gives a mixture efficiency

$$\eta_M=\tfrac{1}{2}(\eta_G+\eta)=\tfrac{1}{2}(\tfrac{2}{3}+1)=0.83\ . \tag{13}$$

This important result of the model has been derived in the general case as the requisite efficiency for testing locally real models that are in agreement with quantum theory subject to the use of low-efficiency detectors [7].

Further progressive detector improvement to the extreme limit of $\eta_G\to1$ requires complete convergence with $\eta\to1$. In this limit of high-efficiency detectors, the model predicts that Eq. (10) will be

$$\frac{R(\theta)}{R_0}=\tfrac{1}{3}C(\theta)\approx\tfrac{1}{3}\cos^2\theta\ . \tag{14}$$

Inequality (12) then has a minimum value set by Eq. (14). These results represent testable consequences of the model when higher efficiency detectors are used.

However, the model also can be tested with existing low-efficiency detectors. For example, if the EPR apparatus is used without analyzers, quantum theory predicts

$$R_L = R_T f\eta, \quad R_0 = R_T f\eta^2$$

as the observed singles rate at the left detector and the observed coincidence rate, respectively. The corresponding quantities predicted by the model are

$$R_L = R_T f\eta_M = R_T f\tfrac{1}{2}(\eta_G + \eta) = 0.83 R_T f\eta ,$$

$$R_0 = R_T f\eta_G\eta = 0.67 R_T f\eta^2$$

[see Eq. (13)]. The disparate ratios

$$[R_0/R_L]_{QT} = \eta, \quad [R_0/R_L]_{\text{model}} = 0.8\eta \tag{15}$$

and calibration of detector efficiency η, independently performed using a pure full-complement photon source, permit experimental exclusion of quantum theory or the model.

In the context of the model, it is instructive to examine the factorization assumption [3] $\mathcal{P}_{LR}(\lambda,\theta) = \mathcal{P}_L(\lambda,\theta_L)\mathcal{P}_R(\lambda,\theta_R)$, where $\theta = \theta_R - \theta_L$, which gives the familiar form of Bell's equation [2]

$$\mathcal{P}_{LR}(\theta) = \int \rho(\lambda)\mathcal{P}_{LR}(\lambda,\theta)d\lambda = \int \rho(\lambda)\mathcal{P}_L(\lambda,\theta_L)\mathcal{P}_R(\lambda,\theta_R)d\lambda . \tag{16}$$

Although (16) and (3) differ in that they are computed in K and K', respectively, the particular choice of reference frame is not significant since $\theta = \theta_R - \theta_L$ is frame independent. Furthermore, the various factors in (3) readily are grouped to give analogous forms to $\rho(\lambda)$ [normalization factor in (1)] and left and right singles probabilities in the integrand of (16). Nevertheless, there remains a fundamental incompatibility between (16) and (3). The photon detection probability on the left, $\mathcal{P}_L(\lambda,\theta_L)$, is the sum of detection probabilities for leftward-moving γ_G's and γ_E's [with a similar expression for $\mathcal{P}_R(\lambda,\theta_R)$]. Then

$$\begin{aligned}\mathcal{P}_{LR}(\theta) &= \int \rho(\lambda)[\mathcal{P}_{L,G}(\lambda,\theta_L)+\mathcal{P}_{L,E}(\lambda,\theta_L)][\mathcal{P}_{R,E}(\lambda,\theta_R)+\mathcal{P}_{R,G}(\lambda,\theta_R)]d\lambda \\ &= \int \rho(\lambda)\mathcal{P}_{L,G}(\lambda,\theta_L)\mathcal{P}_{R,E}(\lambda,\theta_R)d\lambda + \int \rho(\lambda)\mathcal{P}_{L,E}(\lambda,\theta_L)\mathcal{P}_{R,G}(\lambda,\theta_R)d\lambda \\ &\quad + \int \rho(\lambda)\mathcal{P}_{L,G}(\lambda,\theta_L)\mathcal{P}_{R,G}(\lambda,\theta_R)d\lambda + \int \rho(\lambda)\mathcal{P}_{L,E}(\lambda,\theta_L)\mathcal{P}_{R,E}(\lambda,\theta_R)d\lambda .\end{aligned}$$

The first two integrals on the right are comparable to those in (3), but the last two are physically inadmissible in the model in that they relate to correlated pairs of two γ_G's and two γ_E's, respectively. The model, as a consequence of the asymmetry of correlated photons, does not admit factorization (nor does quantum theory [3]) and is not subject to Bell's equation (16).

The model also provides a natural violation of the apparently plausible no-enhancement additional assumption [3]. Using low-efficiency detectors, an incident γ_G photon ($\pi/3$ arc) is detected with an efficiency of $\frac{2}{3}\eta$. If an analyzer is then interposed with its polarization axis oriented to transmit a γ_G, that γ_G collapses to a single packet γ_g in the analyzer and emerges as a γ_e ($\pi/2$ arc). The resultant detection efficiency is naturally enhanced up to η by the presence of the analyzer.

The model, in addition to providing a rational physical basis for violating the additional assumptions of factorization and no enhancement, is distinguished from the diversity of other possible models of local reality (e.g., Ref. [1]) by construction from Malus's law without any arbitrary constants and the testable consequences of Eqs. (12), (14), and (15).

[1] A. Fine, Synthèse **50**, 279 (1982); M. Ferrero and E. Santos, Phys. Lett. A **116**, 356 (1986); F. Selleri and A. Zeilinger, Found. Phys. **18**, 1141 (1988); S. Pascazio, In *Quantum Mechanics versus Local Realism, The Einstein-Podolsky-Rosen Paradox*, edited by F. Selleri (Plenum, New York, 1988); T. W. Marshall and E. Santos, Found, Phys. **18**, 185 (1988); Phys. Rev. A **39**, 6271 (1989); M. Ferrero, T. W. Marshall, and E. Santos, Am. J. Phys. **58**, 683 (1990); V. L. Lepore and F. Selleri, Found. Phys. Lett. **3**, 203 (1990).

[2] J. S. Bell, Physics (N.Y.) **1**, 195 (1964).

[3] J. F. Clauser and M. A. Horne, Phys. Rev. D **10**, 526 (1974).

[4] K. R. Popper, *Quantum Theory and the Schism in Physics* (Rowman and Littlefield, Totowa, NJ, 1982).

[5] J. F. Clauser and A. Shimony, Rep. Prog. Phys. **41**, 1881 (1978), and references therein; A. Aspect, J. Dalibard, and G. Royer, Phys. Lett. **49**, 1804 (1982).

[6] A. Einstein, B. Podolsky, and N. Rosen, Phys. Rev. **47**, 777 (1935).

[7] A. Garg and N. D. Mermin, Phys. Rev. D **35**, 3831 (1987).